Role of Terminal Nonhomologous Domains in Initiation of Human Red Cell Spectrin Dimerization†

Sandra L. Harper, Gillian E. Begg,‡ and David W. Speicher*

The Wistar Institute, Philadelphia, Pennsylvania 19104

Received April 17, 2001; Revised Manuscript Received June 8, 2001

ABSTRACT: Human erythrocyte spectrin is an antiparallel heterodimer comprised of a 280 kDa α subunit and a 246 kDa β subunit which further associates into tetramers in the red cell membrane cytoskeleton. Lateral association of the flexible rodlike monomers involves a multiple-step process that is initiated by a high affinity association near the actin-binding end of the molecule (dimer nucleation site). In this study, recombinant α and β proteins comprising two or four "spectrin type" motifs with and without adjacent, terminal nonhomologous domains were evaluated for their relative contributions to dimer initiation, and the thermodynamic properties of these heterodimer complexes were measured. Sedimentation equilibrium studies showed that in the absence of the heterologous subunit, individual recombinant proteins formed weak homodimers (K_d > 0.3 mM). When 2-motif (α20−21 and β1−2) and 4-motif (α18−21 and β1−4) recombinants lacking the terminal nonhomologous domains were paired with the complementary protein, high affinity heterodimers were formed in sedimentation equilibrium analysis. Both the α20−21/β1−2 complex and the α20−21EF/βABD1−2 complex showed stoichiometric binding with similar binding affinities ($K_d \approx 10$ nM) using isothermal titration calorimetry. The α20−21/β1−2 complex showed an enthalpy of −10 kcal/mol, while the α20−21EF/βABD1−2 complex showed an enthalpy of −13 kcal/mol. Pull-down assays using α spectrin GST fusion proteins showed strong associations between all heterodimer complexes in physiological buffer, but all heterodimer complexes were destabilized by the presence of Triton X-100 and other detergents. Complexes lacking the nonhomologous domains were destabilized to a greater extent than complexes that included the nonhomologous domains. The detergent effect appears to be responsible for the apparent essential role of the nonhomologous domains in prior reports. Taken together, our results indicate that the terminal nonhomologous domains do not contribute to dimer initiation nor are they required for formation of high affinity spectrin heterodimers in physiological buffers.

Erythrocyte spectrin is a large antiparallel heterodimer comprised of an α and β subunit with molecular masses of 280 and 246 kDa, respectively (*1*, *2*). In the red cell membrane cytoskeleton, spectrin is found predominantly as tetramers although small amounts of higher order oligomers are also present (*3*). Electron microscopy images of isolated spectrin dimers show a 100 nm long flexible rodlike molecule with tight associations at the ends of the rods and weaker associations along the central part of the molecule (*4*). In contrast, the contour length of dimers is only about one-third the length of the fully extended molecules in situ (*5*, *6*). The dramatic changes in molecular length and the flexibility of spectrin are generally attributed to most of the basic structure of both subunits of spectrin which consists of tandem, homologous 106 amino acid motifs that fold into triple helical bundles (referred to as helices A, B, and C) as determined by X-ray crystallography (*7*, *8*) and NMR (*9*). α spectrin contains 20 such homologous motifs, an SH3 domain in the ninth motif between helices B and C, a partial motif (a single C helix) at the N-terminus, and C-terminal EF hand domains (*1*). β spectrin contains 16 complete homologous motifs, an N-terminal actin binding domain, a partial motif 17 (helices A and B) and a C-terminal nonhomolgous domain (*2*) that is phosphorylated (*10*). The subunits are arranged antiparallel such that the N-terminus of the β chain is in close proximity to the C-terminus of the α chain thus forming the α/β heterodimer (*11*). A schematic of the spectrin motifs is shown in Figure 1. Heterodimers further associate head-to-head to form tetramers through interaction of the first partial motif of α spectrin with the last partial motif of β spectrin to apparently form complete triple helical bundles (*12*−*14*).

Initial studies in our laboratory using erythrocyte spectrin peptides produced by mild trypsinization showed that only fragments containing approximately four homologous motifs near the N-terminus of β spectrin (β1−4) and about three to four homologous motifs near the C-terminus of α spectrin (α18−21) were capable of forming heterodimeric complexes (*15*). A subsequent study using recombinant peptides and an analytical HPLC gel filtration binding assay demonstrated that the smallest β peptide capable of high affinity dimerization contained the first two homologous motifs (β1−2) (*16*). The effects of ionic strength on the mechanism of molecular docking, and the regions of minimal dimer

† This work was supported by NIH grants HL38794 and NCI core Grant CA10815.

* To whom correspondence should be addressed. Phone: (215) 898-3972. Fax: (215) 898-0664. E-mail: speicher@wistar.upenn.edu.

‡ Present address: Victor Chang Cardiac Research Inst., St. Vincent's Hospital, Darlinghurst, Sydney, New South Wales 2010, Australia.

10.1021/bi0107795 CCC: $20.00
Published on Web 07/27/2001

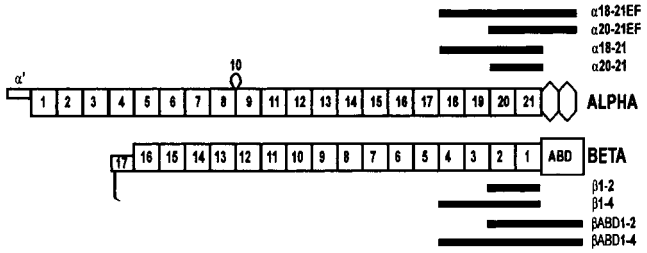

FIGURE 1: Model of the human red cell spectrin antiparallel heterodimer. The numbered rectangles represent homologous motifs of α (1−9, 11−21) and *β* spectrin (1−17). The α′ represents a partial motif at the N-terminus of α spectrin. The ninth α spectrin motif contains an SH3 domain (motif 10) in the loop region between the B and C helices of the triple helical bundle. The hexagons at the C-terminal domain of α spectrin represent the EF hand region. The large box (ABD) at the N-terminus of *β* spectrin represents the actin-binding domain and the "tail" at the C-terminal end is the nonhomologous phosphorylated region. The shaded bars above α spectrin and below *β* spectrin are schematic representations of the constructs used in this study.

nucleation site that interact were subsequently studied (*17*). However, in contrast to our findings, several studies (*18*, *19*) using immunoprecipitation assays of recombinant *Drosophila* spectrin proteins expressed in a reticulocyte lysate system indicated that at least a portion of the adjacent terminal nonhomologous domains were required for formation of high affinity heterodimer complexes. Hence, it was unclear if the discrepancy concerning the potential contributions of the actin binding domain and/or EF hand domains to dimerization were due to the different spectrin isoforms used or the different assay methods used.

In this study, we used sedimentation equilibrium and isothermal titration calorimetry analysis to evaluate the potential contributions of terminal nonhomologous domains to spectrin heterodimerization. Addition of the nonhomologous domains to the recombinant proteins did not enhance the affinity of this interaction. The requirement of these nonhomologous regions for *Drosophila* spectrin dimerization (*18*, *19*) apparently resulted from the assay buffer used in those experiments. That is, spectrin dimer initiation is destabilized by the presence of Triton X-100 and other detergents, and the smallest competent recombinant peptides are somewhat more sensitive to detergents than larger peptides. Complementary 2-motif peptides (α20−21/*β*1−2) were shown to form high affinity heterodimers in physiological buffers by two independent methods, isothermal titration calorimetry and sedimentation equilibrium analysis.

MATERIALS AND METHODS

Expression and Purification of Recombinant Erythrocyte Spectrin Proteins. The polymerase chain reaction was used to amplify the region of interest from erthyrocyte α and *β* spectrin cDNA clones (*1*, *2*) kindly provided by Dr. Bernard Forget. All constructs were expressed as glutathione S-transferase (GST)[1] fusion proteins using either the pGEX-2T vector or pGEX-3X vector (Amersham Pharmacia Biotech). The purification of α18−21, α20−21, *β*1−2, and *β*1−4 has been previously described (*16*, *20*). Recombinant proteins containing the actin binding domain, *β*ABD1−2 (*β* spectrin residues 1−528) and *β*ABD1−4 (*β* spectrin residues 1−743), as well as a α spectrin recombinant containing the EF hand domain, α18−21EF (α spectrin residues 1818−2416), were expressed in a pGEX-2T vector. The α spectrin recombinant containing α20−21EF (α spectrin residues 2033−2416) was expressed in the pGEX-3X vector. Transfected DH5α cells were grown overnight at 37 °C, then diluted 1:20 in LB medium containing 50 *μ*g/mL ampicillin. Cells were grown at 30 °C to an optical density of 0.5−0.7 and induced with 1 mM final concentration of 1-thio-*β*-D-galactopyranoside. Induced cells were allowed to grow for 3 h to a final optical density of approximately 1.0, followed by centrifugation at 4000*g* for 20 min at 4 °C. Cell pellets were immediately frozen and stored at −80 °C until processed for purification. Growth of the transfected *Escherichia coli* at 30 °C resulted in high expression levels with most of the fusion protein in the supernatant fraction after sonication rather than in inclusion bodies. One exception was α20−21, which was expressed at 18 °C in order to obtain a sufficient proportion of the fusion protein in the soluble fraction after sonication. The α20−21EF construct remained in inclusion bodies under all temperature expression conditions tested (18−37 °C); therefore, it was solubilized from inclusion bodies using urea denaturation then refolded using methods as previously described (*21*).

Constructs that contained the EF hand or actin-binding domain were purified from cell lysate supernatants in a manner similar to those previously described for spectrin proteins which did not contain these domains except as noted above (*16*, *17*, *20*). Briefly, the clarified lysate was incubated with reduced glutathione-S-Sepharose for 1 h at 4 °C then washed with 10 mM sodium phosphate, 130 mM NaCl, 5 mM EDTA, and 1 mM 2-ME, pH 7.3. Fusion protein was eluted in 20 mM Tris, 10 mM glutathione, 1 mM 2-ME, 5 mM EDTA, and 0.1 *μ*g/mL pepstatin, pH 8.0. The GST moiety was cleaved from the spectrin proteins using conditions empirically determined for each protein. The α20−21EF fusion protein was cleaved using Factor Xa at an enzyme-to-substrate ratio (*μ*g/*μ*g) of 1:100 for 4 h at 25 °C. The *β*ABD1−2 and *β*ABD1−4 proteins were cleaved with thrombin after addition of NaCl to a final concentration of 0.15 M at an enzyme-to-substrate ratio (units/*μ*g) of 1:1500 and 1:1000, respectively, for 3 h at 37 °C. After cleavage, the proteases were inhibited by addition of PMSF (0.3 mM final concentration). Samples were dialyzed against 10 mM sodium phosphate, 130 MM NaCl, 5 mM EDTA, 0.15 mM PMSF, 1 mM 2-ME, pH 7.3, then reapplied to the glutathione Sepharose 4B column equilibrated in the same buffer. The recombinant spectrin sample was collected as the unbound fraction. Samples were concentrated with a Centriprep concentrator (Millipore) and further purified by gel filtration on a HiLoad Superdex 200 column (60 × 2 cm Amersham Pharmacia) equilibrated with 10 mM sodium phosphate, 130 mm NaCl, 1 mM EDTA, 0.15 mM PMSF, and 1 mM 2-ME pH 7.4. The inserts of all recombinant vectors were analyzed by automated DNA sequencing to verify sequence integrity after PCR amplification.

[1] Abbreviations: GST, glutathione *S*-transferase; PMSF, phenylmethanesulfonyl fluoride; LB, luria broth; HPLC, high-performance liquid chromotography; TCEP, tris(2-carboxyethyl)phosphine hydrochloride; ITC, isothermal titration calorimetry; 2-ME, 2-mercaptoethanol; MALDI-MS, matrix-assisted laser desorption/ionization mass spectrometry; PAGE, polyacrylamide gel electrophoresis; DOC, deoxycholic acid.

Analytical Ultracentrifugation. Spectrin nucleation site recombinants were analyzed using sedimentation equilibrium in a Beckman XL-I analytical ultracentrifuge. Samples were concentrated and buffer was exchanged immediately prior to analytical ultracentrifuge experiments using two analytical (7.8 mm × 300 mm) HPLC gel filtration columns ($G3000SW_{XL}$ + $G2000SW_{XL}$ Tosohaus) in series or two Superdex 200 HR 10/30 (10 × 300 mm Amersham Pharmacia) in series equilibrated in 10 mM sodium phosphate, 130 mM NaCl, 1 mM EDTA, 0.15 mM PMSF, and 1 mM TCEP, pH 7.4. For heterodimeric complexes, equal molar amounts of monomer were mixed together and incubated on ice for 30 min then concentrated using a Centricon concentrator (Millipore) prior to gel filtration. All data was collected using interference optics and cells were assembled with 12 mm Epon double sector Yphantis style centerpieces and sapphire windows. All sample volumes were 110 μL. A water blank scan was taken immediately before each experiment to correct for window distortion in the fringe displacement data (*22*). Three different initial loading concentrations of samples were used for each experiment. In some cases, multiple speeds or temperatures were also used. In these cases, the sample was allowed to reach equilibrium at the lowest speed or temperature, followed by analysis at the second speed or temperature. Fringe displacement data was collected every 4−6 h until equilibrium was reached as determined from comparison of successive scans using the MATCH ver. 7 program.[2]

Data were edited using the REEDIT ver. 9 program[2] and analyzed using the NONLIN ver. 3 program[2] (*23*). Data from all loading concentrations were fitted globally. The reduced molecular weight of the protein is defined as $\sigma = M(1 - \bar{v}\rho)\omega^2/RT$, where M is the sequence molecular weight, $\bar{v}$ is the partial specific volume of the protein, ρ is the solvent density, ω is the angular velocity in radians/s, R is the gas constant, and T is the temperature in kelvin. The program SEDNTERP[2] was used to calculate M and $\bar{v}$ from the amino acid composition of the recombinant proteins as well as ρ for the solvent. Since the difference in σ for each component in the heterodimeric complex as analyzed in this study is $(\sigma_\alpha - \sigma_\beta) \leq 0.6$ at the speeds evaluated, the reaction can be modeled as that of an ideal monomer−dimer association, using the weight-average molecular weight of the two peptides (*24*). A minimum of three data sets from different initial loading concentrations was fitted simultaneously. The data were fitted well by either an ideal single species model or an ideal monomer−dimer model. Examination of the residuals and minimization of the variance determined goodness of fit. The monomer−dimer association constants returned by the NONLIN program were converted to the molar scale using the sequence molecular weight of the proteins and a specific fringe displacement of 3.26 fringes L g (*24*).

Isothermal Titration Calorimetry. Titration experiments were conducted using an MCS isothermal titration calorimeter (ITC) from MicroCal, Inc. equilibrated at 30 °C. Samples for titration calorimetry were dialyzed against 10 mM sodium phosphate, 130 mM NaCl, 1 mM 2-ME, pH 7.4. Prior to the experiment, samples were degassed under vacuum for 5 min. The sample cell was then filled with the final dialysate (used as a control) or protein at a concentration of 3−5 μM. The cell was then titrated with 10−20 aliquots (5−10 μL each) of sample at 5 min intervals. The reaction was stirred at 400 rpm throughout the experiment. Data analysis was performed using the ORIGIN ver. 3.2 data analysis software provided with the instrument. The control experiment was subtracted from the experimental data to correct for heat of dilution of titrant into buffer. The area under each injection spike was integrated and fitted using nonlinear least-squares regression analysis.

Determination of Stoke's Radius. A Superdex 200 HR 10/30 (10 × 300 mm, Amersham Pharmacia Biotech) gel filtration column maintained at 4 °C was equilibrated in 10 mM sodium phosphate, 130 mM NaCl, 1 mM EDTA, 0.15 mM PMSF, 0.05% azide, pH 7.4, at a flow rate of 0.5 mL/min. Protein standards with known Stokes' radii were injected individually onto the column to determine a standard curve (*25*). Each of the spectrin recombinants was then injected onto the column and elution times were used to determine Stokes' radii from the standard curve of known proteins. For evaluation of α/β complexes, an equal molar ratio of each component was mixed together, allowed to reach equilibrium by incubation on ice for 30 min, and then injected onto the columns as described above.

GST-Pull-Down Binding Assays. In GST fusion protein pull down assays, α GST fusion proteins were mixed with various molar ratios of β recombinant proteins in a final volume of 250 μL in 10 mM sodium phosphate, 130 mM NaCl, 5 mM 2-ME, pH 7.4. Heterodimer complexes were allowed to reach equilibrium by incubation on ice for 30 min. Various buffers were tested by adding an equal volume of buffer containing two times the final desired detergent concentration. Final buffer compositions were 10 mM sodium phosphate, 130 mM NaCl, 5 mM 2-ME, pH 7.4 with no detergent; 1% Triton X-100; or 1% Triton X-100, 1% DOC, and 0.1% SDS. Samples were then added to 100 μL of glutathione Sepharose 4B in a Millipore 0.22 μm microfuge filter unit and gently mixed for 1 h at 4 °C. After incubation, the samples were centrifuged for 2 min and the filtrate was collected as the unbound sample. The bound fraction was eluted after a 5 min incubation at room temperature in 500 μL of 0.2% SDS. Bound and unbound fractions were evaluated using Coomassie blue stained 8% SDS−PAGE gels (*26*).

A similar technique was used to perform competition experiments. In these experiments an equal molar amount (usually 250 pmol) of α GST fusion protein and a complementary β recombinant protein were mixed with 0, 125, 250, 500, or 1000 pmol of the various β proteins used in this study. In some other experiments, β1−4 was metabolically labeled with ^{35}S during the protein expression and binding experiments were performed as described above. In addition to SDS gels, liquid scintillation counting was performed on the bound and unbound fraction to determine the portion of labeled protein bound to the α fusion protein.

RESULTS

Purification and Characterization of Spectrin Recombinant Proteins. The role of the actin-binding domain and the EF

[2] MATCH, REEDIT, and NONLIN are available from the Analytical Ultracentrifugation Facility at the University of Connecticut via the FTP site. The program SEDNTERP was written by T. Laue, J. Hayes, and J. Philo, and is available on the RASMB web site.

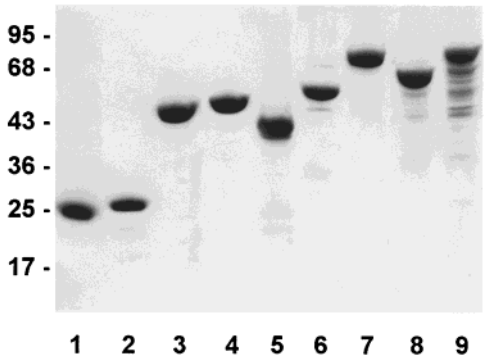

FIGURE 2: Coomassie blue stained 10% Tris-tricine SDS gel of the purified recombinants used in this study. Each lane contains 2 μg of purified protein. Lane 1, α20−21; lane 2, β1−2; lane 3, α18−21; lane 4, β1−4; lane 5, α20−21EF, lane 6, βABD1−2; lane 7, βABD1−4; lane 8, GSTα18−21; lane 9, GSTα18−21EF.

hand motifs in heterodimer assembly and the thermodynamic properties of alternative α/β complexes were evaluated. Figure 1 shows a schematic representation of recombinant proteins used in this study. The phasing (start and stop sites) of each recombinant corresponds to the boundaries of triple helical bundles as defined by crystallographic data (*7*) or as previously determined for the N-terminus of the first homologous β motif (*16*). Recombinant proteins were purified as GST fusion proteins, separated from the GST moiety by enzymatic cleavage followed by rechromatography on a glutathione column, and purified to homogeneity by HPLC gel filtration prior to use. GST fusion proteins used for pull-down assays were purified by glutathione sepharose and HPLC gel filtration. The purity and homogeneity of all proteins was assessed by SDS−PAGE (Figure 2). Protein integrity was confirmed by N-terminal sequencing and MALDI mass analysis, and potential irreversible aggregation of purified samples was measured before use with analytical HPLC gel filtration (data not shown).

The α20−21EF construct was initially cloned into a pGEX-2T vector, however, MALDI mass spectrometry analysis of the purified protein showed a mass smaller than expected. N-terminal sequence analysis together with the observed mass showed that thrombin cleaved the protein at a site near the C-terminal. Subsequently, the α20−21EF cDNA was cloned into a pGEX-3X vector and the expressed protein was cleaved with Factor Xa. Using this expression system, a protein with the expected mass was obtained by MALDI mass spectrometry. This protein could be purified in low yield (2 mg of fusion protein/L of bacterial culture) from the lysate supernatant or in high yield (30 mg of fusion protein/L of bacterial culture) when extracted from the pellet fraction. Expression of the protein at low temperatures (18−25 °C) did not prevent incorporation of the fusion protein into inclusion bodies. Protein purified from either the supernatant fraction or from inclusion bodies behaved similarly in binding assays, showed identical resistance to protease cleavage, and had the same Stokes' radius, indicating the protein was properly refolded (data not shown). Since protein was purified from inclusion bodies in much higher yields, this method was used for subsequent analysis.

Sedimentation Equilibrium Analysis of Spectrin Constructs. Purified proteins were rechromatographed on analytical

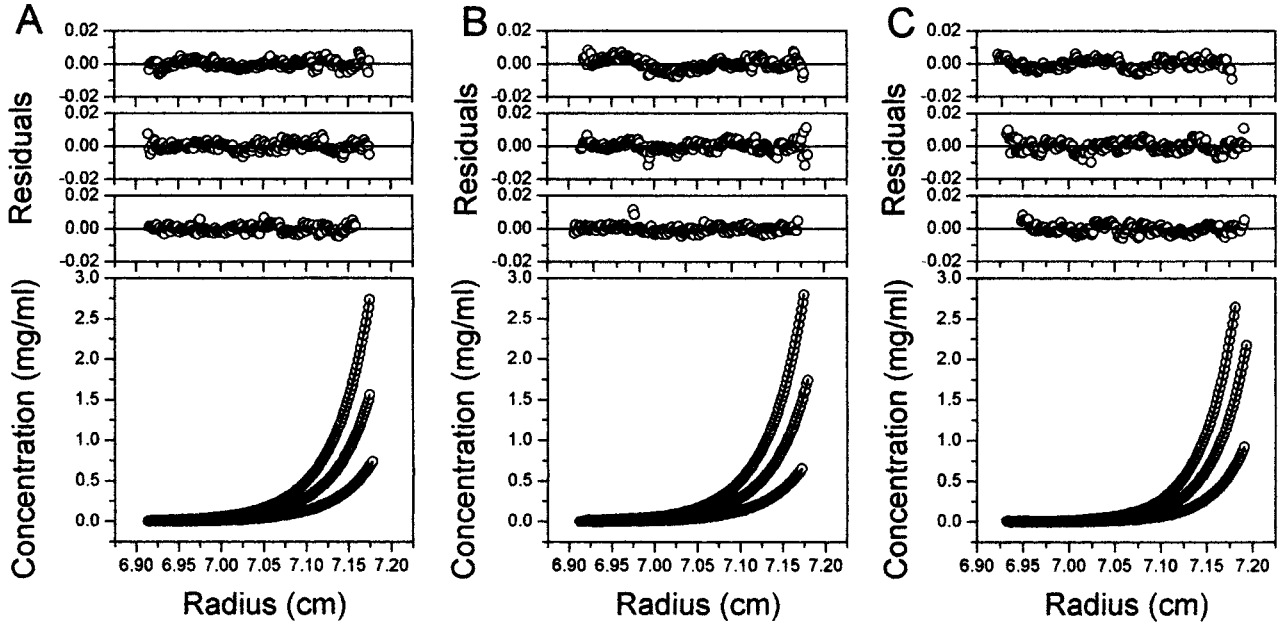

FIGURE 3: Representative sedimentation equilibrium analyses of 2-motif dimer nucleation site recombinants. (A) (Lower panel) α20−21 at three initial loading concentrations (1.0, 0.5, and 0.25 mg/mL) in 10 mM sodium phosphate, 130 mM NaCl, 1 mM EDTA, 0.15 mM PMSF, and 1 mM TCEP, pH 7.4, at 31 800 rpm and 30 °C. The raw data (circles) and the global fit for a monomer−dimer equilibrium with a K_d of 1.3 mM are shown (lines). (Upper panel) The residuals of the fitted curves to the data points for each concentration from highest to lowest (top to bottom, respectively). (B) (Lower panel) β1−2 at three initial loading concentrations (0.9, 0.45, and 0.225 mg/mL) in 10 mM sodium phosphate, 130 mM NaCl, 1 mM EDTA, 0.15 mM PMSF, 1 mM TCEP, pH 7.4 at 30 600 rpm and 30 °C. The raw data (circles) and the global fit of a monomer−dimer equilibrium with a K_d of 1.1 mM are shown (lines). (Upper panel) The residuals of the fitted curves to the data points for each concentration from highest to lowest (top to bottom, respectively). (C) (Lower panel) α20−21/β1−2 at three initial loading concentrations (0.8, 0.4, and 0.2 mg/mL) in 10 mM sodium phosphate, 130 mM NaCl, 1 mM EDTA, 0.15 mM PMSF, 1 mM TCEP, pH 7.4 at 22 000 rpm and 30 °C. The raw data (circles) and the global fit of a single species (lines) with an observed molecular mass of 52 729 Da are shown (expected heterodimer mass = 54 869 Da). (Upper panel) The residuals of the fitted curves to the data points for each concentration from highest to lowest (top to bottom, respectively).

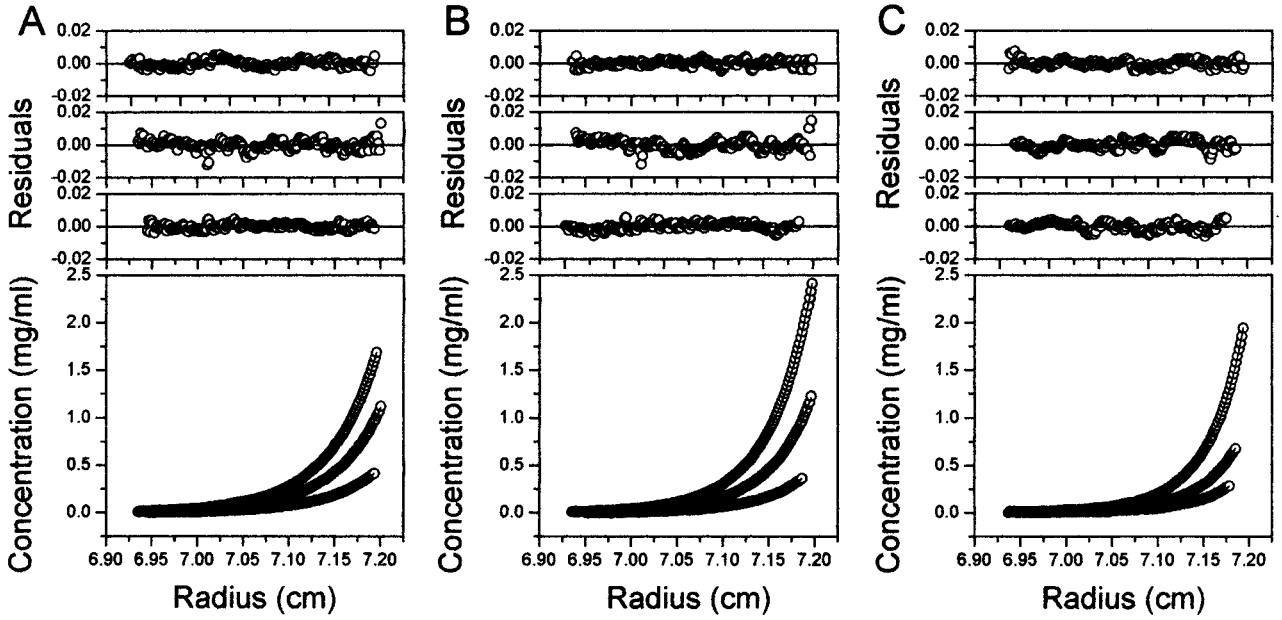

FIGURE 4: Sedimentation equilibrium analysis of 2-motif spectrin recombinants with EF hand and actin-binding domains. (A) (Lower panel) α20−21EF at three initial loading concentrations (0.6, 0.3, and 0.15 mg/mL) in 10 mM sodium phosphate, 130 mM NaCl, 1 mM EDTA, 0.15 mM PMSF, 1 mM TCEP, pH 7.4, at 22 700 rpm and 30 °C. The raw data (circles) and the global fit of a monomer−dimer equilibrium with a K_d of 1.2 mM are shown (lines). (Upper panel) The residuals of the fitted curves to the data points for each concentration from highest to lowest (top to bottom, respectively). (B) (Lower panel) βABD1−2 at three initial loading concentrations (0.8, 0.4, and 0.2 mg/mL) in 10 mM sodium phosphate, 130 mM NaCl, 1 mM EDTA, 0.15 mM, PMSF, 1 mM TCEP, pH 7.4, at 20 000 rpm and 30 °C. The raw data (circles) and the global fit of a monomer−dimer equilibrium with a K_d of 0.4 mM are shown (lines). (Upper panel) the residuals of the fitted curves to the data points for each concentration from highest to lowest (top to bottom, respectively). (C) (Lower panel) analysis of a α20−21EF/βABD1−2 1:1 complex at three initial loading concentrations (0.7, 0.35, and 0.175 mg/mL) in 10 mM sodium phosphate, 130 mM NaCl, 1 mM EDTA, 0.15 mM PMSF, 1 mM TCEP, pH 7.4, at 17 000 rpm and 30 °C. The raw data (circles) and the global fit of a monomer−dimer equilibrium with a K_d of 516 nM are shown (lines). (Upper panel) The residuals of the fitted curves to the data points for each concentration from highest to lowest (top to bottom, respectively).

Table 1: Sedimentation Equilibrium of Spectrin Nucleation Recombinants

experiment	fitting model[a]	K_d 30 °C (mM)	RMS ($\times 10^{-3}$)[b] 30 °C	K_d 4 °C (mM)	RMS ($\times 10^{-3}$)[b] 4 °C
individual recombinants					
α20−21	monomer−dimer	1.3	7.2	NA[c]	
β1−2	monomer−dimer	1.1	8.7	NA[c]	.
α18−21	monomer−dimer	0.34	1.6	NA[c]	
β1−4	monomer−dimer	0.34	6.6	NA[c]	
α20−21EF	monomer−dimer	1.21	8.0	0.23	9.2
βABD1−2	monomer−dimer	0.41	8.2	0.21	8.5
α/β complexes					
α20−21/β1−2	dimer	ND[d]	8.8	ND[d]	8.9
α18−21/β1−4	dimer	ND[d]	9.2	ND[d]	8.5

[a] A global fitting model was applied to each sample for three different initial loading concentrations. In some cases multiple speeds were simultaneously fitted as well. [b] RMS, root-mean-square. [c] NA, not analyzed. [d] ND, not determined. Data were fit to a single species model.

HPLC gel filtration columns immediately prior to analysis by sedimentation equilibrium to remove minor amounts of aggregates that may have formed after initial purification. Equal molar amounts of complementary α and β subunits were mixed together to form heterodimeric complexes, incubated on ice for 30 min, concentrated using a Centricon concentrator to approximately 8 mg/mL then injected onto the HPLC gel filtration columns. Fractions from the leading edge of the α/β complex peak were used in sedimentation equilibrium experiments to ensure that there was no contamination with inactive monomers. Initially, each of the individual spectrin recombinant proteins was analyzed since some spectrin recombinants were capable of forming large irreversible aggregates (*20*). Also, the single-motif α14 *Drosophila* spectrin protein forms a high affinity homodimer with a well-folded rearrangement (*27*). In the current sedimentation equilibrium studies, homodimers could not be distinguished from heterodimers and would affect data analysis if homodimer and heterodimer dissociation constants would be similar.

Representative data for individual motifs and heterodimeric complexes of 2-motifs and 2-motifs with the nonhomologous domains are shown in Figures 3 and 4. Table 1 lists the monomer−dimer dissociation constants for each individual protein recombinant. No significant differences in the binding affinities were detected between 4 and 30 °C. Individual α or β spectrin recombinants could be fitted by a model describing a weak reversible monomer−dimer equilibrium (K_d = 0.3−1.3 mM). The heterodimeric complexes of α18−21/β1−4 and α20−21/β1−2 fit best to models for a single species with molecular weights corresponding to α/β dimers. When the highest concentration data set was removed,

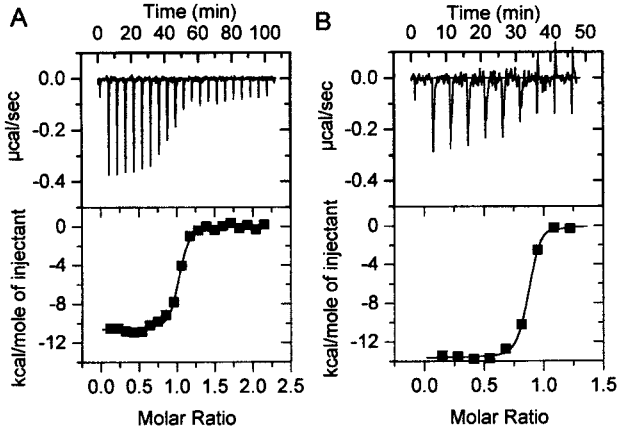

FIGURE 5: Representative isothermal titration calorimetry profiles of dimer nucleation site recombinants at 30 °C. (A) (Upper panel) The baseline subtracted titration curve of α20−21 (3.8 mg/mL) injected as 20 × 5 μL aliquots at 5 min intervals into the titration cell containing β1−2 (0.14 mg/mL). Both samples were dialyzed into 10 mM sodium phosphate, 130 mM NaCl, 1 mM 2-ME, pH 7.4, and degassed 5 min prior to loading the samples. (Lower panel) The blank corrected integrated areas for the peaks were plotted against the molar ratio of [α20−21]/[β1−2]. The data were fitted using a nonlinear least-squares method (line). (B) (Upper panel) The baseline subtracted titration curve of α20−21EF (4.4 mg/mL) injected as 12 × 7 μL aliquots at 5 min intervals into βABD1−2 (0.24 mg/mL). Both samples were dialyzed into 10 mM sodium phosphate, 130 mM NaCl, 1 mM 2-ME, pH 7.4, and degassed 5 min prior to loading the samples. (Lower panel) The blank corrected integrated areas for the peaks was plotted against the molar ratio of [α20−21EF]/[βABD1−2]. The data were fitted using a nonlinear least-squares method (line).

monomer−dimer K_ds of ∼20 nM were estimated. Surprisingly, the α20−21EF and βABD1−2 complex exhibited weaker and variable dimer affinities ($K_d \approx 600 \pm 300$ nM, average of three independent experiments). Since the ITC studies described below indicated low nanomolar affinities for this complex, it was apparently somewhat unstable over the time course of the sedimentation equilibrium experiments.

Isothermal Titration Calorimetry. Heterodimerization of α and β spectrin recombinants was further characterized using isothermal titration calorimetry. This method was used to verify binding stoichiometry and to more precisely determine dissociation constants of heterodimeric complexes. As shown above, sedimentation equilibrium experiments of most complexes allowed only estimation of an upper limit for K_ds due to the small amount of free monomers present in these experiments. Isothermal titration calorimetry was also used to determine enthalpy of reaction for each group of recombinant proteins. Representative titration curves and nonlinear least-squares fits for two-motif recombinants with and without the EF hands and actin-binding domain are shown in Figure 5. All reactions showed similar K_ds in the low nanomolar range and heats of reaction of about −10 kcal/mol for α20−21/β1−2 and about −13 kcal/mol for α20−21EF/βABD1−2 in 10 mM sodium phosphate, 130 mM NaCl, and 1 mM 2-ME, pH 7.4. Table 2 summarizes values obtained for representative experiments using different recombinant pairings.

Determination of Stokes' Radius. The Stokes' radii data for individual recombinants and α/β complexes are shown in Table 3. The individual α spectrin recombinants have slightly larger hydrodynamic radii compared to their complementary β subunit recombinant, despite the fact that the β recombinants have slightly larger masses. When heterodimeric complexes are formed, only a modest increase in Stokes' radius is observed relative to the α recombinant alone. These results are most consistent with an in-register lateral alignment of motifs, i.e., α21 aligns with β1, α20 aligns with β2, etc.

Table 2: Isothermal Titration Calorimetry of Spectrin Nucleation Site Recombinants

complex formed[a]	N	K_A (M^{-1})	ΔH (kcal/mol)	K_d (nM)
α20−21/β1−2	0.93 ± 0.02	(4.8 ± 2.4) × 10^7	−10.3 ± 0.3	21
	0.99 ± 0.02	(13.6 ± 1.7) × 10^7	−9.4 ± 0.4	7.4
α20−21EF/	0.81 ± 0.01	(13.7 ± 1.9) × 10^7	−13.6 ± 0.1	7.3
βABD1−2	0.79 ± 0.01	(28.6 ± 9.1) × 10^7	−13.4 ± 0.2	3.5

[a] Titrant is listed first followed by the protein in the cell. All experiments were performed in 10 mM sodium phosphate, 130 mM NaCl, and 1 mM 2-ME pH 7.4. Results of two representative independent experiments for each complex are shown.

Table 3: Hydrodynamic Radii of Spectrin Nucleation Site Recombinants

recombinant	2-motif (nm)	2-motif + nonhomologous (nm)	4-motif (nm)
α	3.0	3.7	4.1
β	2.8	3.9	4.0
α/β	3.5	4.3	4.4

Fusion Protein Pull-Down Binding Assays. The ability to form heterodimer complexes was further explored by evaluating the capability of β recombinants to form complexes with complementary α GST fusion proteins under different experimental conditions. A physiological buffer comprised of 10 mM sodium phosphate, 130 mM NaCl, and 5 mM 2-ME, pH 7.4, was the standard buffer used in all experiments. In parallel experiments, detergents such as Triton X-100, DOC, and SDS were used alone or in combination to obtain buffer conditions similar to those used in the *Drosophila* spectrin dimerization assays (*18*, *19*). In several representative experiments α GST fusion proteins (250 pmol) were mixed with 250 pmol of different β proteins and allowed to reach equilibrium. The complexes were then precipitated with glutathione Sepharose. Under all conditions used, the fusion protein was essentially completely bound to the glutathione Sepharose. A representative experiment is shown in Figure 6. In the presence of physiological buffer without detergents, both α GST fusion proteins were able to form tight associations with a complementary β recombinant. However, these interactions were substantially destabilized by the presence of Triton X-100 which reduced heterodimer association by about 50%. In the presence of 10 mM sodium phosphate, 130 mM NaCl, 5 mM 2-ME, 1% Triton X-100, 1% DOC, and 0.1% SDS, pH 7.4, the detergent conditions used in a previous spectrin dimerization assay (*18*), the majority of the complementary β protein was in the unbound fraction. This experiment clearly showed that the presence of detergent severely disrupted these heterodimeric complexes.

Competition GST-pull down experiments were performed using equal molar amounts of GSTα18−21EF and βABD1−4 with 0−4-fold excess of different β spectrin recombinants as competitors. In all experiments, β1−2 and β1−4 were

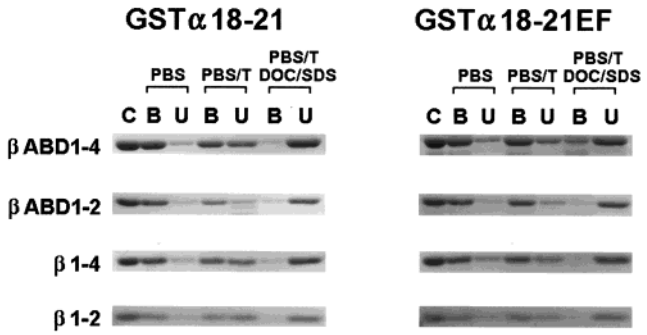

FIGURE 6: GST-pull down assay of nucleation site recombinants. Binding of GSTα18−21 or GSTα18−21EF to a series of β recombinants. For each panel, control (C), bound (B), and unbound (U) fractions are shown for each series of beta peptides, β1−2, β1−4, βABD1−2, or βABD1−4 using three alternative buffer conditions: PBS-10 mM sodium phosphate, 130 mM NaCl, 5 mM 2-ME, pH 7.4; PBS/T-PBS buffer with 1% Triton X-100, pH 7.4; and PBS/T/DOC/SDS−PBS buffer with 1% Triton X-100, 1% DOC, 0.1% SDS, pH 7.4.

capable of competing with the βABD1−4 protein. In another series of experiments, GSTα20−21EF was mixed with ^{35}S-β1−4 and equal molar amounts of various β recombinant proteins were added as competitors using the different buffer/detergent conditions described above and 0.1% BSA was included as a blocking agent. In these experiments, proteins that contained the actin-binding domain were able to compete slightly more effectively than those that did not, although results varied from experiment to experiment (data not shown).

DISCUSSION

Previous studies by our laboratory showed that the first two homologous motifs of erythrocyte β spectrin and the last two homologous motifs of α spectrin were the minimum regions capable of forming stable heterodimeric complexes (*17*). Other studies using *Drosophila* spectrin showed that regions of the actin-binding domain and EF hand motifs were necessary for dimerization to occur (*18*, *19*). However, it was unclear whether these observed differences were due to the different assay methods used to evaluate binding or the different spectrin isoforms used in the respective studies. The aim of the current study was to fully characterize the dimerization of erythrocyte spectrin using several biophysical and biochemical techniques to measure binding affinities. Using sedimentation equilibrium and isothermal titration calorimetry, this study unambiguously demonstrated that the nonhomologous domains were not necessary for dimerization and that these nonhomologous domains did not enhance heterodimer binding affinity in physiological buffers with out detergent.

Sedimentation equilibrium analysis of individual recombinants showed that all recombinants used here formed weak homodimers with low affinities (K_ds ≈ 1 mM). No differences in K_d values were observed between 4 and 30 °C. Since these interactions were readily reversible and weaker they did not influence the much stronger heterodimer thermodynamic analysis.

During the course of these studies, some α spectrin recombinants were observed to be sensitive to oxidation and could form disulfide adducts when stored in the presence of 2-ME or glutathione adducts when stored in the presence of glutathione. Formation of these disulfide adducts resulted in decreased and often variable affinities of heterodimer complexes (data not shown). Presumably, disulfide adducts with these weak reducing reagents were forming with exposed unusually reactive cysteine residues on the protein surface involved in subunit−subunit contact. Therefore, effective reduction of cysteine adducts proved to be critical since, when it was omitted, some heterodimer protein preparations exhibited erroneously weak association constants that were an order of magnitude or more lower than expected. For example, when the α20−21/β1−2 complex was analyzed by sedimentation equilibrium in the absence of reducing agents, the dissociation constants were typically about 1 μM. An unrelated study demonstrated that the strong reducing agent, TCEP, which cannot form disulfide adducts, can effectively dissociate disulfide adducts (*28*). Hence, TCEP was used in all sedimentation equilibrium experiments described in this report to prevent oxidation of any free sulfhydryl groups in the spectrin recombinants.

Isothermal titration calorimetry was used to further explore the binding affinities between two-motif α and β recombinants containing EF hand and actin-binding domains, respectively, compared with two motif α and β recombinants lacking the terminal nonhomologous domains (Table 2). The stoichiometry of reaction (N) for each experiment was in the range of 0.8−1.1, indicating a 1:1 molar ratio of reactants as expected. All data shown here utilized freshly purified proteins since samples stored for more than about 7 days would sometimes yield N values less than 0.8. When such recently purified proteins were used, the average K_d for the α20−21/β1−2 complex was 14 nM consistent with the sedimentation equilibrium experiments. There was no significant effect of the nonhomologous domains on binding affinity since the average K_d for the α20−21EF/βABD1−2 of 5.4 nM was within experimental error of the value for the 2-motif complex. However, The nonhomologous domains do appear to contribute an additional 3 kcal/mol. This observed difference in enthalpy might be due to an error in the α20−21EF protein concentration since ΔH is measured in terms of [titrant]/[ligand] and stoichiometries for these reactions were typically ∼0.8 (see Table 2). However, an erroneous α20−21EF concentration is not a likely basis for the enthalpy difference since this would require that the concentration was consistently 20% higher than measured using absorbance at 280 nm and molar extinction coefficients calculated from the SEDNTERP program. Most errors in protein concentration determinations tend to over estimate rather than underestimate protein content. Hence, the more likely explanation for the N values of ∼0.8 is that the concentration of the βABD1−2 was overestimated or about 20% of the βABD1−2 was inactivated by shear forces from the stirred cell. Since errors in the protein concentration in the reaction cell do not affect the enthalpy value, the observed 3 kcal/mol contribution to enthalpy of association suggests that conformation changes in the nonhomologous domains occur upon association but do not substantially contribute to the affinities of this complex.

Sedimentation equilibrium analysis of α20−21EF/βABD1−2 interaction consistently showed weaker binding affinities (≥300 nM) then 2-motif dimers even in the presence of a high concentration of strong reducing agent (10 mM TCEP). Independent analyses of these complexes using an HPLC gel filtration assay as described in earlier

dimerization studies (*16*) showed that the K_d was <100 nM (data not shown) consistent with the low nanomolar K_d observed in the ITC experiments. The most likely explanation for the weaker and somewhat variable binding affinities of the α20−21EF/βABD1−2 complex using sedimentation equilibrium compared with these alternative techniques was that one or both proteins were not fully stable over the longer time course of the experiment (≤2 h for a titration or HPLC gel filtration experiment, compared with about 32 h for sedimentation equilibrium). The instability of one or both recombinants in sedimentation equilibrium experiments could be due to subtle proteolysis that could not be detected by 1D SDS gels, adsorption to the cell housing or another unknown inactivation mechanism. Consistent with this limited stability of at least one of these recombinants is the fact that the *N* value in isothermal titration calorimetry experiments was consistently around 0.8 despite the shorter time scale of ITC (see above). The GST-pull down competition assays further support the high affinity nature of the α20−21EF/βABD1−2 interaction since these proteins exhibited similar binding affinities to those proteins lacking these domains when physiological buffer without detergents was used. Taken together, these multiple biochemical and biophysical analysis showed that α20−21EF and βABD1−2 form high affinity heterodimers with K_ds essentially identical to α20−21 and β1−2, and the weaker affinities measured by sedimentation equilibrium for the α20−21EF/βABD1−2 complex are most likely due to instability of one or both recombinants under these conditions.

In contrast to the studies of *Drosophila* spectrin dimerization (*18*, *19*), the results of this study demonstrate that the actin-binding domain and EF hand region do not contribute to high affinity dimerization in erythrocyte spectrin. Since the *Drosophila* spectrin study used an antibody immunoprecipitation assay in the presence of Triton X-100, DOC, and SDS, we used a GST pull-down assay to test the effects of these detergents on erythrocyte spectrin dimerization. The experiments described herein strongly suggest that the apparent requirement for the nonhomologous domains for dimerization of *Drosophila* spectrin were due to the detergents used in that study rather than isoform differences. Although all erythrocyte spectrin recombinants bound the heterologous GST fusion proteins, addition of Triton X-100 decreased binding of all constructs by approximately half. In the presence of Triton X-100, DOC, and SDS, conditions similar to the one used for the immunoprecipitation assays in the *Drosophila* study, binding was essentially abolished for all constructs except βABD1−4 and α18−21EF. Interestingly, when a blocking agent (0.1% BSA) was included in the Triton X-100, SDS, DOC containing buffer, binding was still not observed for any α−β pair that did not contain the actin-binding domain or EF hand motifs; however, constructs containing the actin-binding domain and EF hand regions did exhibit appreciable binding under these conditions, duplicating the results observed with *Drosophila* spectrin recombinants. Apparently, BSA in these experiments reduces the detergent perturbation of dimeric complexes by sequestering some of the detergent, thereby reducing but not eliminating inhibition of dimerization. As described above, these detergents destabilize all complexes, although the effects on the larger proteins with the nonhomologous domains were less severe and substantial association was observed for these complexes. Attenuation of the detergent inhibition of dimerization by the larger proteins on addition of BSA suggests that the total protein mass/detergent ratios determine the degree of dimerization inhibition. Clearly, the detergent effects on all recombinants without the nonhomologous domains are sufficient to explain the differing conclusions of prior *Drosophila* spectrin (*18, 19*) and our human red cell spectrin studies.

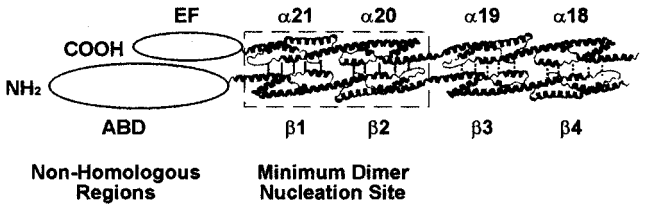

FIGURE 7: Model of the spectrin dimer initiation site region. The small oval represents the C-terminal EF hand region of α spectrin and the larger oval represents the N-terminal actin-binding domain of β spectrin. The in-register lateral alignment of α20−21 to β1−2 (minimum dimer nucleation site) is thought to be initially directed by long-range electrostatic attraction followed by stabilization of the interaction by hydrophobic and van der Waals interactions (—) where the AB faces of these triple helical motifs dock with each other. This high affinity interaction positions adjacent homologous motifs in proximal locations where very weak affinities (- - -) pair additional motifs throughout the remainder of the dimer.

Recent publication of a two-motif α-actinin central rod domain (*29*) shows an antiparallel homodimer in which the motifs pair in an aligned fashion. Since the spectrin nucleation site motifs share a high sequence homology with α-actinin, it is likely that they would pair in a similar manner such that α21 pairs with β1, α20 with β2, etc. Electrostatic modeling of α20 and β2 support an aligned pairing for the nucleation site recombinant proteins where the AB faces of the helices are in contact with one another (*17*). The small increases observed in the Stokes' radius of the heterodimeric complexes compared to the individual α and β recombinants further support an in-register lateral pairing of α21-β1, α20-β2, etc., in the dimerization of spectrin (Figure 7).

A comprehensive model for the mechanism of spectrin dimerization is suggested by combining the results of this study with prior analyses (*15*−*17*). Correct orientation of intact α chains with the N-terminal region of nascent β chains, possibly partially synthesized chains bound to ribosomes, occurs through long-range complementary electrostatic interactions of the AB helical faces of α21 with β1 and α20 with β2. These longer range interactions probably ensure that the correct homologous motifs dock with each other, and the resulting strong interaction of the minimum dimer initiation regions (α20−21 and β1−2) involves hydrophobic and van der Waals interactions in addition to salt bridges. This initial association aligns the α EF hand domain and the β actin-binding domains next to each other (Figure 7) but direct interactions of these domains, if any, must be very weak and do not significantly contribute to the overall heterodimer interaction. The initial high affinity association of α20−21 with β1−2 is followed by subsequent weak associations of proximal α and β motifs, i.e., α19 to β3, α18 to β4, α17 to β5, etc, until all available motifs have laterally paired. These additional weaker associations moderately increase the affinity of the dimeric complex and maintain the close lateral association of the subunits under physiological conditions.

ACKNOWLEDGMENT

We thank Dr. Bernard Forget (Yale University, New Haven, CT) for providing the spectrin cDNA clones. We also thank David Reim for N-terminal sequence analysis and Kaye Speicher for MALDI-MS analysis.

REFERENCES

1. Sahr, K. E., Laurila, P., Kotula, L., Scarpa, A. L., Coupal, E., Leto, T. L., Linnenbach, A. J., Winkelmann, J. C., Speicher, D. W., Marchesi, V. T., Curtis, P. J., and Forget, B. G. (1990) *J. Biol. Chem. 265*, 4434−4443.
2. Winkelmann, J. C., Chang, J.-G., Tse, W. T., Scarpa, A. L., Marchesi, V. T., Forget, B. G. (1990) *J. Biol. Chem. 265*, 11827−11832.
3. Liu, S. C., Derick, L. H., and Palek, J. (1987) *J. Cell Biol. 104*, 527−536.
4. Shotton, D. M., Burke, B. E., and Branton, D. (1979) *J. Mol. Biol. 131*, 303−329.
5. McGough, A. M., and Josephs, R. (1990) *Proc. Natl. Acad. Sci. U.S.A. 87*, 5208−5212.
6. Ursitti, J. A., Pumplin, D. W., Wade, J. B., and Bloch, R. J. (1991) *Cell Motil. Cytoskel. 19*, 227−243.
7. Yan, Y., Winograd, E., Viel, A., Cronin, T., Harrison, S. C., and Branton D. (1993) *Science 262*, 2027−2030.
8. Grum, V. L., Li, D., MacDonald, R. I., and Mondragon, A. (1999) *Cell 98*, 523−535.
9. Pascual, J., Pfuhl, M., Walter, D., Saraste, M., and Nilges, M. (1997) *J. Mol. Biol. 273*, 740−751.
10. Harris, H. W., Jr., and Lux, S. E. (1980) *J. Biol. Chem. 255*, 11512−11520.
11. Speicher, D. W., Morrow, J. S., Knowles, W. J., and Marchesi, V. T. (1982) *J. Biol. Chem. 257*, 9093−9101.
12. Tse, W. T., Lecomte, M. C., Costa, F. F., Garbarz, M., Feo, C., Boivin, P., Dhermy, D., and Forget, B. G. (1990) *J. Clin. Invest. 86*, 909−916.
13. Speicher, D. W., DeSilva, T. M., Speicher, K. D., Ursitti, J. A., Hembach, P., and Weglarz, L. (1993) *J. Biol. Chem. 268*, 4227−2030.
14. Kennedy, S. P., Weed, S. A., Forget, B. G., and Morrow, J. S. (1994) *J. Biol. Chem. 269*, 11400−11408.
15. Speicher, D. W., Weglarz, L., and DeSilva, T. M. (1992) *J. Biol. Chem. 267*, 14775−14782.
16. Ursitti, J. A., Kotula, L., DeSilva, T. M., Curtis, P. J., and Speicher, D. W. (1996) *J. Biol. Chem. 271*, 6636−6644.
17. Begg, G. E., Harper, S. L., Morris, M. B., and Speicher, D. W. (2000) *J. Biol. Chem. 275*, 279−3287.
18. Viel, A., and Branton, D. (1994) *Proc. Natl. Acad. Sci. U.S.A. 91*, 10839−10843.
19. Veil, A., Gee, M. S., Tomooka, L., and Branton, D. (1998) *Biochim. Biophys. Acta 1384*, 396−404.
20. Wilmotte, R., Harper, S. L., Ursitti, J. A., MarJchal, J., Delaunay, J., and Speicher, D. W. (1997) *Blood 90*, 4188−4196.
21. Harper, S., and Speicher, D. W. (1998) In *Current Protocols in Protein Science* (Coligan, J. E., Dunn, B. M., Ploegh, H. L., Speicher, D. W., and Wingfield, P. T., Eds.) pp 6.6.1−6.6.21, John Wiley & Sons, New York.
22. Yphantis, D. A. (1964) *Biochem. 3*, 297−317.
23. Johnson, M. L., Correia, J. J., Yphantis, D. A., and Halvorson, H. R. (1981) *Biophys. J. 36*, 575−588.
24. Luckow, E. A., Lyons, D. A., Ridgeway, T. M., Esmon, C. T., and Laue, T. M. (1989) *Biochem. 28*, 2348−2354.
25. Harper, S., and Speicher, D. W. (1998) In *Current Protocols in Protein Science* (Coligan, J. E., Dunn, B. M., Ploegh, H. L., Speicher, D. W., and Wingfield, P. T., Eds.) pp 7.10.1−1.10.15, John Wiley & Sons, New York.
26. Laemmli, U. K (1970) *Nature 227*, 680−685.
27. Ralston, G., Cronin, T. J., and Branton, D. (1996) *Biochemistry 35*, 5257−5263.
28. Begg, G. E., and Speicher, D. W. (1999) *J. Bio. Technol. 10*, 17−20.
29. Dijinovic-Carugo, K., Young, P., Gautel, M., and Saraste, M. (1999) *Cell 98*, 537−536.

BI0107795